PYROLYSIS OF THE POLYMER COAL: STRUCTURE AND KINETICS

BY

AMIR ATTAR AND GREGORY G. HENDRICKSON

DEPARTMENT OF CHEMICAL ENGINEERING
UNIVERSITY OF HOUSTON
HOUSTON, TEXAS 77004

1. INTRODUCTION

A kinetic model which predicts the rate of formation of gaseous products produced during coal pyrolysis has been developed. The basis assumptions of the kinetic model are similar to those of Attar (1) for the kinetics of coal liquefaction in a hydrogen donor solvent. The main assumption is that different coals consist of the same organic functional groups and that the differences between coals are due to the different concentrations of the functional groups. The functional groups most important in forming gaseous products are hydroaromatic hydrogen, methyl groups, ethyl groups and oxygen functionalities, i.e., carboxyl groups, carbonyl groups, phenols and ether linkages. The products of coal pyrolysis are to a large extent determined by the initial concentration of each of the above mentioned functionalities.

The chemistry and thermodynamics of functional group reactions in coal are, to a first-order approximation, independent of the particular coal (2). It is also plausible to assume that the reaction rate of each functional group is independent of the particular coal and only dependent upon the regent, the reactive group and the temperature. Thus the kinetic parameters, the activation energy and the frequency factor, are assumed to be independent of the particular coal. Arrhenius dependence of the rate constants are assumed.

The rate of product generation appears to be controlled by thermal decomposition of the coal (3), thus the rate of chemical reaction is assumed to be the controlling rate. Mass transfer effects have been neglected. The bond breaking process has been assumed to proceed by a free radical mechanism for which the steady state assumption can be applied. The free radicals can then form stable products by combination reactions with other radicals or by hydrogen abstraction reactions. Secondary reactions, other than the water-shift reaction, have been neglected. The water-shift reaction has been assumed to proceed to equilibrium.

The kinetic model incorporates all of the above assumptions into a set of rate equations for the transformations of the various functional groups. Isothermal

kinetics or a constant heating rate can be used. The rate expressions are integrated numerically using a semi-implicit third order Runge-Kutta method with the initial functional group distribution in a coal as the boundary condition. After each integration step, the water-shift reaction is shifted to equilibrium.

2. KINETIC MODEL

The kinetic model which has been developed is based on the premise that free radicals are released from the coal matrix and then undergo combination reactions or hydrogen abstraction reactions to form stable products. The free radicals which are released from the coal matrix include hydrogen atoms, methyl groups and ethyl groups. Each of these radicals is released from the coal matrix according to the first-order reaction

$$S - R \rightarrow S\cdot + R\cdot$$

where $S\cdot$ is the radical remaining in the solid phase to later take place in tar forming or char forming reactions and $R\cdot$ is either $H\cdot$, $\cdot CH_3$ or $\cdot C_2H_5$. Once formed, the free radicals can either undergo a second-order combination reaction of the type

$$R_i\cdot + R\cdot_j \rightarrow R_iR_j$$

where i and j refer to any of the above mentioned radicals and R_iR_j is the stable product, or they can abstract hydrogen from the coal matrix to result in the stable product RH. The hydrogen abstraction reaction is a second-order reaction of the type.

$$R\cdot + S'H \rightarrow S'\cdot + RH$$

The reactions involving free radicals can produce the gaseous products H_2, CH_4, C_2H_6, C_3H_8 and C_4H_{10}. Once a stable product is formed, cracking reactions to form lower molecular weight products are not assumed to occur. This assumption is approximately correct in that the components most likely to crack, i.e., C_3H_8 and C_4H_{10}, are produced only in minor quantities. Ethylene production is assumed to occur as a resulted of the unimolecular decomposition of ethyl radicals according to the reaction

$$\cdot C_2H_5 \rightarrow C_2H_4 + H\cdot$$

Other reactions which must be considered involve oxygen functional groups. The oxygen functional groups are responsible for the formation of CO_2, CO and H_2O. Carbon dioxide is assumed to occur due to decarboxylation reactions involving carboxyl groups. Carbon monoxide is assumed to be formed from two sources. The low temperature peak is thought to result from elimination of quinonic-carbonyl groups. The higher temperature peak is thought to result from the cleavage of ether linkages. Water formation is due to reactions involving phenol groups. Each of these products is assumed to be formed according to first-order kinetics.

Finally, the gas phase reaction

$$H_2O + CO \rightleftharpoons CO_2 + H_2$$

must be considered. This reaction has been shown to be approximately in equilibrium in the products from coal pyrolysis (4,5) and is the only "secondary" reaction considered in the kinetic model. After each integration step the product composition is shifted to equilibrium values for the above reaction. The water-shift reaction is the "tie" between the effective rate of production of each of the products involved and the actual rate of production of each of these products.

3. MATHEMATICAL DEVELOPMENT

As previously mentioned, the rate of formation of $H^{\cdot}$, $\cdot CH_3$, $\cdot C_2H_5$, CO_2, CO and H_2O is assumed to be described by first-order kinetics. The rate of formation of each of these species can thus be described by the equations

$$\frac{dR_i}{dt} = k_i (S\text{-}R)_i$$

where R_i is the "gas" phase concentration of the i-th species and $(S\text{-}R)_i$ is the concentration of that species remaining attached to the coal matrix. When R_i is $H^{\cdot}$, $\cdot CH_3$ or $\cdot C_2H_5$ the radical can be stabilized by combination reactions with other radicals or by hydrogen abstraction reactions. Both of the above reactions are assumed to follow second-order kinetics with the exception of two hydrogen atoms combining to form molecular hydrogen which requires a third body for stabilization of the product. Thus the rate of formation of stable products is described by equations 3.2 through 3.7.

$$\frac{d(H_2)}{dt} = k_1 (H^{\cdot})^2 (M) + k_2 (H^{\cdot})\ S\text{-}H \qquad 3.2$$

$$\frac{d(CH_4)}{dt} = k_3 (H^{\cdot}) (\cdot CH_3) + k_4 (\cdot CH_3) (S\text{-}H) \qquad 3.3$$

$$\frac{d(C_2H_6)}{dt} = k_5 (\cdot CH_3)^2 + k_7 (\cdot C_2H_5) (H^{\cdot}) + k_8 (\cdot C_2H_5) (S\text{-}H) \qquad 3.4$$

$$\frac{d(C_3H_8)}{dt} = k_6 (\cdot CH_3) (\cdot CH_3) (\cdot C_2H_5) \qquad 3.5$$

$$\frac{d(C_4H_{10})}{dt} = k_9 (\cdot C_2H_5)^2 \qquad 3.6$$

$$\frac{d(C_2H_4)}{dt} = k_{10} (\cdot C_2H_5) \qquad 3.7$$

In equations 3.2 - 3.7 the radical combination reactions occur with no activation energies. Hydrogen abstration rate constants and the ethyl decomposition rate constant assume Arrhenius behavior. The rate constants associated with equations 3.1 - 3.7 are listed in Tables 3.1 - 3.3. Along with

the rate constants associated with the functional group transformations are activation energies for the decomposition reactions of the polymers assumed to characterize the bond breaking process involved in the functional group transformations.

In order to integrate the given rate equations the radical concentrations must be available. The radical concentrations have been obtained with radical balances and the assumption that the steady-state approximation is valid.

According to Benson (6), the steady-state assumption has been shown to be valid if the total radical concentration is negligible compared to the reactant and product concentrations. The radical concentrations are usually negligible in the integration procedure which has been incorporated. The utility of the steady-state assumption is that it converts differential equations into algebraic equations which can then be solved for the radical concentrations. The radical balances are presented in equations 3.8 - 3.10.

$$\frac{d(H\cdot)}{dt} = \frac{d(S-H)}{dt} - 2k_1 (H\cdot)^2 (M) - k_2 (H\cdot) (S-H) - k_3 (\cdot CH_3) (H\cdot) - k_7 (\cdot C_2H_5) (H\cdot) + k_{10} (\cdot C_2H_5) = 0 \qquad 3.8$$

$$\frac{d(\cdot CH_3)}{dt} = \frac{d(S-CH_3)}{dt} - k_3 (\cdot CH_3)(H\cdot) - k_4 (\cdot CH_3) (S-H) - 2k_5 (\cdot CH_3)^2 - k_6 (\cdot CH_3) (\cdot C_2H_5) = 0 \qquad 3.9$$

$$d(\cdot C_2H_5) = d(S-C_2H_5) - k_6 (\cdot CH_3) (\cdot C_2H_5) - k_7 (\cdot C_2H_5) (H\cdot) - k_8 (\cdot C_2H_5) (S-H) - 2k_9 (\cdot C_2H_5)^2 - k_{10} (\cdot C_2H_5) = 0 \qquad 3.10$$

In the kinetic model the radical balances are solved by successive approximations until a solution is obtained within allowable error.

Table 3.1

Functional Group Decomposition Rate Constants

Functional Group	A(sec^{-1})	E(kcal/mole)
-H	73.0	25.0
$-CH_3$	16.7	18.0
C_2H_5	16.7×10^6	31.4
-COOH	550.0	19.5
-C=O	55.0	18.0
-O-	2500.0	30.2
-OH	1.05×10^{15}	

Model Compound	E(kcal/mole)	Reference
Tetralin (-H)	22.0	11
Polybenzyl ($-CH_3$)	53.0	12
Polyacrylic Acid (1-COOH)	27.0	13
Poly (2,6-dimethyl-1,4-phenylene ether)(OH)	57.0	14

Table 3.2

Radial Reaction Rate Constants

Reaction	k(cc/mole sec)	Reference
$H\cdot + H\cdot + M \rightarrow H_2 + M$	8.9×10^{15}*	15
$\cdot CH_3 + H\cdot \rightarrow CH_4$	6.0×10^{12}	16
$\cdot CH_3 + \cdot CH_3 \rightarrow$	3.16×10^{13}	17
$\cdot CH_3 + \cdot C_2H_8$	2.51×10^{12}	18
$\cdot C_2H_5 + H\cdot \rightarrow C_2H_6$	3.63×10^{12}	17
$\cdot C_2H_5 + \cdot C_2H_5 \rightarrow C_4H_{10}$	1.0×10^{13}	18
$\cdot C_2H_5 \rightarrow C_2H_4 + H\cdot$	$k = 2.7 \times 10^{14} \exp(-40{,}900/RT)\,sec^{-1}$	19

Table 3.3

Hydrogen Abstraction Reactions Rate Constants

Reaction	log A(cc/mole sec)	E(kal/mole)	Reference
$H\cdot + S\text{-}H \rightarrow H_2 + S\cdot$	10.61	5.4	20
$\cdot CH_3 + S\text{-}H \rightarrow CH_4 + S\cdot$	10.61	8.0	estimated
$\cdot C_2H_5 + S\text{-}H \rightarrow C_2H_6 + S\cdot$	13.5	4.4	estimated

4. RESULTS

The concentrations of the various gaseous products produced during coal pyrolysis and the rate of formation of these gases can be obtained by employing the kinetic model previously described. The results of modeling the prolysis of two typical coals are described in this section. In both cases, the results from the kinetic model have been compared to experimental data obtained from the literature. The published data is that of Campbell and Stephens (7) and Makino and Toda (8,9).

Campbell and Stephens (7) pyrolyzed Wyodak subbituminous coal at temperatures between 110° and 1000°C. A constant heating rate of 3.33°C/mm was used to heat a sample weighing 50 gm and consisting of particles sized between 10 mesh and 6 mesh. Argon was used as a carrier gas to sweep the gaseous products to a mass spectrometer for quantitative determination of the product composition. Experimentally obtained gas evolution curves are compared with the curves obtained from the kinetic model in Figures 1-4. A material balance is presented in Table 4.1. The experimental carbon dioxide yield was estimated by graphical integration of the experimental rate of evolution curve.

It is interesting to compare the initial functional group distribution with the calculated gaseous yield. It can be seen that all of the methyl groups go into the formation of methane and all of the ethyl groups form ethane. Radical combination reactions other than with hydrogen are negligible. Also, if enough hydrogen is subtracted from the initial hydrogen concentration to account for methane and ethane formation, the yield of molecular hydrogen would be 61.3 cm^3/gm compared to the calculated yield of 98.9 cm^3/gm. This apparent discrepancy, along with the observation that more carbon dioxide is in the products than there is carboxyl groups in the feed is the result of the water-shift reaction. For this case, the overall effect of the water-shift reaction is a shift in the direction

$$H_2O + CO \rightarrow CO_2 + H_2$$

It should be noted that all of the calculated water yield is formed from the phenols. If some moisture is initially present and the water-shift reaction proceeds in the same direction as before, the calculated hydrogen yield could be made to approach the experimental yield.

The methane and ethane yields are presented in Figure 1. It can be seen that first-order kinetics do not adequately describe the rate of methane formation, especially at the tail end of the rate curve. This observation is in agreement with Fitzgerald and Van Krevelen (10) who said that the rate of methane formation does not decrease as rapidly as predicted by first-order kinetics. Based on kinetic arguments, they postulated a second source of methane to be the reaction

$$C(s) + 2H_2 \rightarrow CH_4$$

The second methane source which is postulated here is the rupture of alicyclic rings. Methane has been shown to be produced upon the pyrolysis of tetralin (11), thus alicyclic rings are known to be able to form methane upon pyrolysis.

Table 4.1

Characterization of Wyodak Subbituminous Coal

Coal Composition		Gaseous Equivalent of the Initial Functional Group Distribution		Gaseous Yield (cm^3/gm)		
Component	Wt.%	Group	Conc.(cm3/gm)	Component	Experimental	Model
C	66.76	-H	196.4	H_2	124.8	98.9
H	5.25	$-CH_3$	67.2	CH_4	67.2	67.2
O	16.99	$-C_2H_5$	6.6	C_2H_6	6.63	6.6
N	1.11	-COOH	18.2	CO_2	48	54.9
S	0.74	C =O	26.1	CO	45.9	63.6
		-O-	73.1	H_2O	---	66.8
		-OH	101.9			

The rupture of alicyclic rings should be more important in lower ranked coals since the concentration alicyclic ring is postulated to decrease with an increase in rank.

A comparison between calculated and experimental volatilization yields for an anthracite are illustrated in Figures 5-8. Makino and Toda (8,9) used a flow-type high pressure reactor and a constant heating rate of 3.3° C/min up to a final temperature of 900°C in their experiments. A constant flowrate of helium was used to sweep gaseous products out of the reactor and into a high speed chromatograph for analysis. Argon was used as a carrier gas in separate experiments for the determination of hydrogen. The experimental curves reproduced herein were obtained by graphical integration of experimental rate curves. An estimated 10-15% error in the calculated yields is possible. A material balance is included in Table 4.2.

Table 4.2

Characterization of Omine Anthracite

Coal Composition		Gaseous Equilvalent of the Initial Functional Group Distribution				
Component	Wt.%	Group	Conc.(cm^3/gm)	Component	Experimental	Model
C	93.2	-H	150.1	H_2	138.7	71.8
H	3.3	$-CH_3$	10.8	CH_4	11.3	10.8
O	1.2	$-C_2H_5$	0.05	C_2H_6	-----	0.05
N	1.7	-COOH	0.0094	CO_2	1.52	1.23
S	0.7	C =O	0.76	CO	3.18	7.36
		-O-	7.81	H_2O	------	7.16
		-OH-	8.25			

The main observations are:

1. All the methyl and ethyl groups form methane and ethane respectively. For this case, first order kinetics can adequately describe the methane evolution rate. This observation is another point in favor of the secondary methane source required for lower ranked coals being the cleavage of alicyclic rings.

2. The water-shift reaction shifts in the direction

$$H_2O + CO \rightarrow CO_2 + H_2$$

The calculated carbon dioxide yield shown in Figure 7 is a direct result of the water-shift reaction. A negligible amount of the carbon dioxide evolved is the result of decarvoxylation reactions.

5. MODEL LIMITATIONS

The limitations of the model are:

1. The model does not predict tar yields.
2. The model is limited to low pressure applications due to the neglect of secondary reactions.
3. The rate constants for the release of the free radicals from the coal are applicable to low heating rates. A heating rate of as high as 60° C/sec will shift the calculated initial temperature for methane formation away from the experimental temperature by approximately 10°C.
4. Correlations predicting the initial functional group distribution are limited to coals containing between approximately 70% C and 92% C.

BIBLIOGRAPHY

1. Attar, A., Prep. Div. Fuel Chem., A.C.S., 23 (4), 169 (1978).

2. Messenger, L. and Attar, A., Fuel, 58 (9), 655 (1979).

3. Anthony, D. B. and Howard, J. B., A.I.Ch.E.J., 22 (4), 625 (1976).

4. Suuberg, E. M., W. A. Peters and J. B. Howard, I.E.C., Proc. Des. Div., 17 (1), 37 (1978).

5. Wen, C. Y. and T. Z. Chaung, I.E.C., Proc. Des. Div., 18 (4), 684 (1979).

6. Benson, S. W., "Thermochemical Kinetics", Wiley, N. Y., 1976, p. 229.

7. Campbell, J. H. and D. R. Stephens, A. C. S. Prep. For 1976 meeting in San Francisco.

8. Makino, M. and Y. Toda, Fuel, 58, 231 (1979).

9. Makino, M. and Y. Toda, Fuel, 58, 573 (1979).

10. Fitzgerald D. and D. W. Van Krevelen, Fuel, 38, 17 (1959).

11. Bredael, P. and T. H. Vinh, Fuel, 58, 211 (1979).

12. Madorsky, S. L. and S. Straus, J. Res. Nat'l. Bur. Standards, 53 (6), 361.

13. Eisenbert, A. and T. Yokoyama, A. C. S. Div. Polym. Chem., 9 (2), 1408 (1968).

14. Factor, A., J. Polym. Sci., Part A-1, 7, 363 (1969).

15. Kretschmer, C. B. and H. L. Peterson, J. Chem. Phys., 39, (7), 1772 (1963),

16. Mulcahy, M., "Gas Kinetics", Wiley, N. Y., 1973.

17. Kochi, J. K. (ed.), "Free Radicals" Vol. I., John Wiley and Sons, N. Y., 1973, p. 6.

18. Benson, S. W., "Thermochemical Kinetics", Wiley, N. Y., 1976, p. 164.

19. Loucks, L. F. and K. J. Laidler, Canadian J. Chem., 45, 2795, (1967).

20. Denisov, E. T., "Liquid Phase Reaction Rate Constants", I. F. I./Plenum, N. Y., 1974, pp. 286-287.

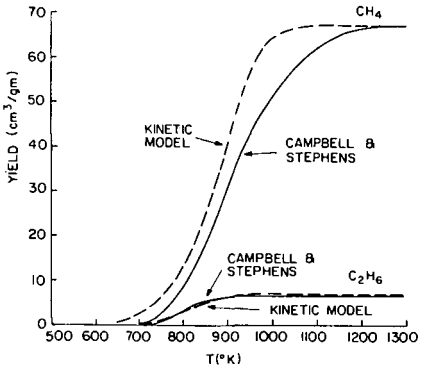

Figure 1. CH_4 and C_2H_6 Ref. (7)

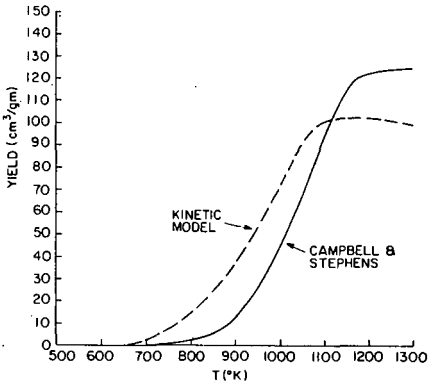

Figure 2. Hydrogen Ref. (7)

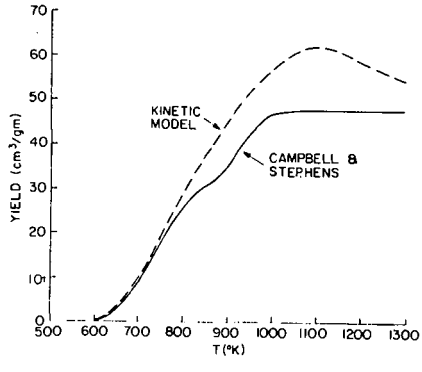

Figure 3. Carbon Dioxide Ref. (7)

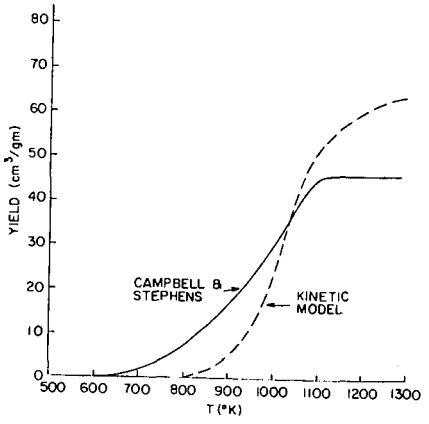

Figure 4. Carbon Monoxide Ref. (7)

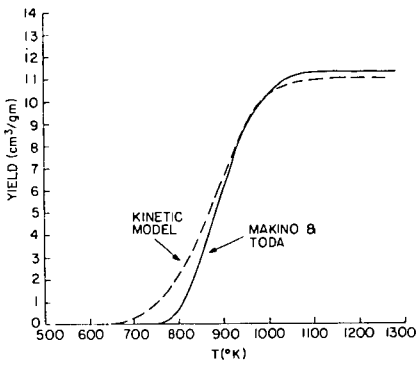

Figure 5. Methane Ref. (8,9)

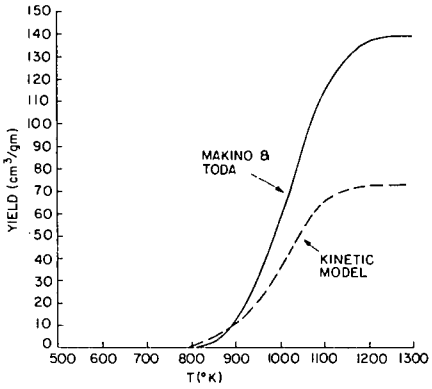

Figure 6. Hydrogen Ref. (8,9)

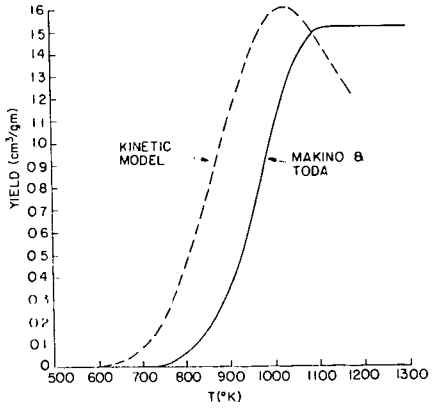

Figure 7. Carbon Dioxide Ref. (8,9)

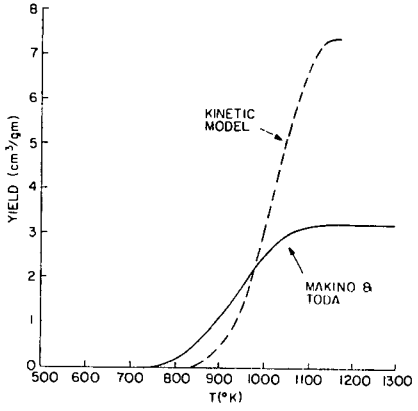

Figure 8. Carbon Monoxide Ref. (8,9